

A TFETI DOMAIN DECOMPOSITION SOLVER FOR ELASTOPLASTIC PROBLEMS

M. ČERMÁK¹, T. KOZUBEK¹, S. SYSALA², J. VALDMAN^{1*}

Centre of Excellence IT4Innovations,
¹VŠB-Technical University of Ostrava,
²Institute of Geonics AS CR, v.v.i., Ostrava,
Czech Republic

March 30, 2022

Abstract

In the paper, we propose an algorithm for the efficient parallel implementation of elastoplastic problems with hardening based on the so-called TFETI (Total Finite Element Tearing and Interconnecting) domain decomposition method. We consider an associated elastoplastic model with the von Mises plastic criterion and the linear isotropic hardening law. Such a model is discretized by the implicit Euler method in time and the consequent one time step elastoplastic problem by the finite element method in space. The latter results in a system of nonlinear equations with a strongly semismooth and strongly monotone operator. The semismooth Newton method is applied to solve this nonlinear system. Corresponding linearized problems arising in the Newton iterations are solved in parallel by the above mentioned TFETI domain decomposition method. The proposed TFETI based algorithm was implemented in Matlab parallel environment and its performance was illustrated on a 3D elastoplastic benchmark. Numerical results for different time discretizations and mesh levels are presented and discussed and a local quadratic convergence of the semismooth Newton method is observed.

1 Introduction

Elastoplastic processes describe behaviour of solid continuum beyond reversible elastic deformations. They are typically described by hysteresis models with a time memory [BS96, Kr96]. The rigorous mathematical analysis of elastoplastic problems and the numerical methods for their solution started to appear in the late 70ies and in the early 80ies by the work of C. Johnson [Jo76, Jo78], H. Matthies [Ma79, Ma79b], V. Korneev and U. Langer [KL84], J. Nečas and I. Hlaváček [NH81] and others. Since then a lot of mathematical contributions to computational plasticity have been written. Here we refer at least to some of them: to the monographs by J. Simo and T. Hughes [SH98] and W. Han and B. Reddy [HR99], to the book of Blaheta [B199], to the habilitation theses by C. Carstensen [C93] and C. Wiensers [Wi00], and to the collection of papers by E. Stein et al. [St03].

In this paper, we focus on the efficient parallel implementation of elastoplastic problems based on the TFETI domain decomposition method. More specifically, we consider an associated elastoplasticity with the von Mises plastic criterion and the linear isotropic hardening law (see e.g. [HR99, B199, NPO08]). The corresponding elastoplastic constitutive model is discretized by the implicit Euler method in time and consequently a nonlinear stress-strain relation is implemented by the return mapping concept (see e.g. [NPO08, ACZ99, B199]). This approach together with the balance equation, the small strain assumption and a combination of the Dirichlet and Neumann boundary conditions leads to the solution of a nonlinear variational equation with respect to the primal unknown displacement in each time step. Such an equation can also be equivalently formulated as a minimization problem with a potential energy functional (see e.g. [GV09, Sy09]).

*corresponding author, email: jan.valdman@vsb.cz

By a finite element space discretization of the one time step problem, we obtain a system of nonlinear equations. The corresponding nonlinear operator is nondifferentiable but strongly semismooth. Therefore, it is suitable to choose the semismooth Newton method for solving the system since the strong semismoothness together with other properties ensure local quadratic convergence. Semismooth functions in finite dimensional spaces and the semismooth Newton method were introduced in [QS93]. In elastoplasticity, the semismoothness was investigated for example in [GV09, SW11, Sy09, Sy12].

In each Newton iteration, it is necessary to solve the respective linearized problem. Different linear solvers including those based on multigrid have been successfully tested in [Wi10, GKLSV11]. Moreover, since the linear systems of equations corresponding to the elastic and elastoplastic problems are spectrally equivalent [KLV04], all preconditioners for elastic problems can be applied to elastoplastic ones as well.

A linear solver considered in this paper is based on a FETI type domain decomposition method enabling its efficient parallel implementation. The standard FETI method (FETI-1) was originally introduced by Farhat and Roux [FR92]. Using this approach, a body is partitioned into non-overlapping subdomains, an elliptic problem with Neumann boundary conditions is defined for each subdomain, and intersubdomain field continuity is enforced via Lagrange multipliers. The Lagrange multipliers are evaluated by solving a relatively well conditioned dual problem of a small size that may be efficiently solved by a suitable variant of the conjugate gradient algorithm. The first practical implementations exploited only the favorable distribution of the spectrum of the matrix of the smaller problem [Ro92], known also as the dual Schur complement matrix, but such algorithm was efficient only with a small number of subdomains. Later, Farhat, Mandel, and Roux introduced a “natural coarse problem” whose solution was implemented by auxiliary projectors so that the resulting algorithm became in a sense optimal [FMR94, RF98]. Here, we use the Total-FETI (TFETI) [DHK06] variant of FETI domain decomposition method, where even the Dirichlet boundary conditions are enforced by Lagrange multipliers. Hence all subdomain stiffness matrices are singular with a-priori known kernels which is a great advantage in the numerical solution. With known kernel basis we can regularize effectively the stiffness matrix without extra fill in and use any standard sparse Cholesky type decomposition method for nonsingular matrices [BDKKM10]. An alternative linear solver based on the Schwarz domain decomposition method with overlapping was introduced by [BG94].

The structure of the paper is as follows: In Section 2, we introduce a quasistatic scheme of a solid mechanics problem. Within this context, we consider the both elastic and elastoplastic models. The elastic model is introduced from the methodical purposes because it is an essential part of the investigated elastoplastic model. After its time discretization we summarize the resulting one time step problem. In Section 3, the finite element space discretization of the one time step problem and its nonlinear algebraic formulation are described in details. The semismooth Newton method is applied to treat this nonlinearity. The TFETI method combined with the projected conjugate gradient algorithm is derived in Section 4 to solve the linearized problems appearing in the Newton iterations. Finally, the algorithm for solving the whole elastoplastic problem is summarized. In Section 5, the performance of the proposed algorithm is illustrated on numerical experiments. Final comments are summarized in Section 6.

2 Elastic and elastoplastic models

In this section, we summarize elastic and elastoplastic models in a quasistatic framework. Firstly, we introduce basic notation and assumptions that will be used for setting the models. Secondly, we describe the linear elastic constitutive model for an isotropic material. Thirdly, we introduce the elastoplastic initial value constitutive model based on the described elasticity, the von Mises yield function, the associated plastic flow rule and the linear isotropic hardening represented by the accumulated plastic strain. Fourthly, we consider time discretization of the constitutive model given by the implicit Euler method. The explicit form of the time discretized elastoplastic operator is introduced.

2.1 Notation and assumptions

Let us consider a deformable body occupying a domain $\Omega \subset \mathbb{R}^3$ with a Lipschitz continuous boundary $\Gamma = \partial\Omega$. We will describe the state of the body during a loading process by the Cauchy stress tensor $\sigma \in S$, the displacement $u \in \mathbb{R}^3$ and the small strain tensor $\varepsilon \in S$. Here $S = \mathbb{R}_{sym}^{3 \times 3}$ is the space of all

symmetric second order tensors. Other variables that are necessary for defining the elastoplastic models will be introduced in Subsection 2.3. More details can be found in [NPO08].

The above variables depend on the spatial variable $x \in \Omega$ and on the time variable $t \in Q = [t_0, t^*]$. The small strain tensor is related to the displacement by the linear relation

$$\varepsilon(u) = \frac{1}{2} (\nabla u + (\nabla u)^T). \quad (1)$$

The equilibrium equation in the quasistatic case reads

$$-\operatorname{div}(\sigma(x, t)) = g(x, t) \quad \forall (x, t) \in \Omega \times Q, \quad (2)$$

where $g(x, t) \in \mathbb{R}^3$ represents the volume force acting at the point $x \in \Omega$ and the time $t \in Q$.

Let the boundary Γ be fixed on a part Γ_U that has a nonzero Lebesgue measure with respect to Γ , i.e. we prescribe the homogeneous Dirichlet boundary condition on Γ_U :

$$u(x, t) = 0 \quad \forall (x, t) \in \Gamma_U \times Q. \quad (3)$$

On the rest of the boundary $\Gamma_N = \Gamma \setminus \Gamma_U$, we prescribe the Neumann boundary conditions

$$\sigma(x, t)n(x) = F(x, t) \quad \forall (x, t) \in \Gamma_N \times Q, \quad (4)$$

where $n(x)$ denotes the exterior unit normal and $F(x, t)$ denotes a prescribed surface forces at the point $x \in \Gamma_N$ and the time $t \in Q$. Geometry of Ω with imposed boundary conditions is depicted in Figure 1. Similarly, we can consider other boundary conditions, for example symmetry and periodic conditions.

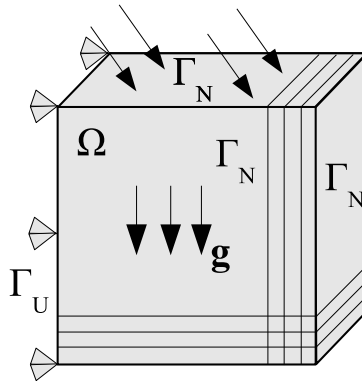


Figure 1: Geometry of the domain Ω with imposed boundary conditions.

For a weak formulation of the investigated problems, it is sufficient to introduce the space of kinematically admissible displacements,

$$V = \{v \in [H^1(\Omega)]^3 : v = 0 \text{ on } \Gamma_U\}. \quad (5)$$

Then the conditions (2)–(4) can be written in a weak sense by

$$\int_{\Omega} \langle \sigma, \varepsilon(v) \rangle_F dx = \int_{\Omega} g^T v dx + \int_{\Gamma_N} F^T v ds \quad \forall v \in V, \forall t \in Q. \quad (6)$$

Here $\varepsilon(v)$ is defined by (1), $\langle \cdot, \cdot \rangle_F$ and $\|\cdot\|_F$ denote the Frobenius scalar product and the corresponding norm on the space S , respectively. We assume that the functions σ, F, g are sufficiently smooth to be the integrals in (6) correctly defined in the Lebesgue sense.

To complete the investigated (generally quasistatic) models, we will prescribe the constitutive relations among the stress, the strain and eventually other variables.

2.2 Elastic model

We consider the elastic constitutive model given by the Hooke law for isotropic material,

$$\sigma = \mathbb{C}\varepsilon = \lambda \text{tr}(\varepsilon)I + 2\mu\varepsilon \quad (7)$$

with the Lamé coefficients λ, μ . For the sake of simplicity, we assume a homogeneous material, i.e. the constant coefficients $\lambda, \mu > 0$. The trace operator of a tensor is denoted by $\text{tr}(\cdot)$ and I denotes the identity.

It will be useful to introduce the volumetric and deviatoric parts of a tensor $\eta \in S$ by

$$\text{vol}(\eta) = \frac{1}{3}\text{tr}(\eta)I, \quad \text{dev}(\eta) = \eta - \text{vol}(\eta). \quad (8)$$

It holds that

$$\langle \text{vol}(\eta), \text{dev}(\xi) \rangle_F = 0, \quad \langle \text{dev}(\eta), \xi \rangle_F = \langle \text{dev}(\eta), \text{dev}(\xi) \rangle_F \quad \forall \eta, \xi \in S. \quad (9)$$

By (9), we can find that the fourth order tensor \mathbb{C} , defined by (7), is symmetric and elliptic, i.e.

$$\langle \mathbb{C}\eta, \xi \rangle_F = \langle \eta, \mathbb{C}\xi \rangle_F, \quad \langle \mathbb{C}\eta, \eta \rangle_F \geq 2\mu\|\eta\|_F^2 \quad \forall \eta, \xi \in S. \quad (10)$$

If we substitute (7) into (6), we obtain for any fixed $t \in Q$ the weak formulation of the elastic problem.

Problem 1 (Elastic problem). Find $u = u(x, t) \in V$ such that

$$a_e(u, v) = \int_{\Omega} g^T v dx + \int_{\Gamma_N} F^T v ds \quad \forall v \in V, \quad (11)$$

where the bilinear form on V reads

$$a_e(w, v) = \int_{\Omega} \langle \mathbb{C}\varepsilon(w), \varepsilon(v) \rangle_F dx, \quad w, v \in V. \quad (12)$$

Note that $a_e(w, v)$ is symmetric and V -elliptic by (10) and the Korn inequality [NH81], i.e.

$$a_e(w, v) = a_e(v, w), \quad \exists c > 0 : a_e(v, v) \geq c\|v\|_V^2 \quad \forall v, w \in V. \quad (13)$$

The mentioned properties of the form a_e insure that the elastic problem (11) has a unique solution $u \in V$, for example by Lax-Milgram lemma [NH81]. Notice that the problem (11) does not depend on the load history, so it is a static problem.

2.3 Elastoplastic initial value constitutive model

In comparison to elasticity, elastoplasticity is time dependent model where the history of loading is taken into account. We will assume associated elastoplasticity with von Mises plastic criterion and linear isotropic hardening law (see e.g. [HR99, Bl99, NPO08]). The elastoplastic initial-value constitutive model consists of the following components:

1. Additive decomposition of the strain tensor into the elastic and plastic parts:

$$\varepsilon = \varepsilon^e + \varepsilon^p. \quad (14)$$

2. Linear elastic law between the stress and the elastic strain:

$$\sigma = \mathbb{C}\varepsilon^e, \quad (15)$$

where the fourth order tensor \mathbb{C} is defined by (7).

3. The von Mises yield function coupled with an isotropic hardening variable κ :

$$\Phi(\sigma, \kappa) = \sqrt{\frac{3}{2}}\|\text{dev}(\sigma)\|_F - (\sigma_y + H_m\kappa) \leq 0, \quad (16)$$

where $\sigma_y, H_m > 0$ denote the initial yield stress and the hardening modulus, respectively.

4. The associated plastic flow rule:

$$\dot{\varepsilon}^p = \dot{\gamma} \frac{\partial \Phi}{\partial \sigma} = \dot{\gamma} \sqrt{\frac{3}{2}} \frac{\text{dev}(\sigma)}{\|\text{dev}(\sigma)\|_F}, \quad \dot{\gamma} \geq 0, \quad (17)$$

where $\dot{\varepsilon}^p$ and $\dot{\gamma}$ denote the time derivative of the plastic strain and the plastic multiplier, respectively.

5. The hardening law based on the accumulated plastic strain rate:

$$\dot{\kappa} = \sqrt{\frac{2}{3}} \|\dot{\varepsilon}^p\|_F = \dot{\gamma}. \quad (18)$$

Notice that the second equality in (18) follows from (17).

6. The loading/unloading conditions:

$$\dot{\gamma} \geq 0, \quad \Phi(\sigma, \kappa) \leq 0, \quad \dot{\gamma} \Phi(\sigma, \kappa) = 0. \quad (19)$$

7. The initial conditions:

$$\varepsilon(x, t_0) = \varepsilon^e(x, t_0) = \varepsilon^p(x, t_0) = \sigma(x, t_0) = 0, \quad \kappa(x, t_0) = 0, \quad x \in \Omega. \quad (20)$$

The weak formulation of the corresponding elastoplastic problem can be found in [HR99]. Here we will only consider a time discretized elastoplastic model.

2.4 Time discretized elastoplastic model

Let us consider the following discretization of the time interval

$$t_0 < t_1 < \dots < t_k < \dots < t_N = t^*.$$

Let us denote $\sigma_k = \sigma_k(x) = \sigma(x, t_k)$, $x \in \Omega$ and similarly for other variables. To approximate the time derivatives, we use the implicit Euler method. However, it is also possible to use for example the Crank-Nicholson scheme. Then by (14) and (15),

$$\dot{\varepsilon}^p(t_{k+1}) \approx \frac{\varepsilon_{k+1}^p - \varepsilon_k^p}{\Delta t_{k+1}} = \frac{\mathbb{C}^{-1}(\sigma_{k+1}^t - \sigma_{k+1})}{\Delta t_{k+1}}, \quad \Delta t_{k+1} = t_{k+1} - t_k, \quad (21)$$

where

$$\sigma_{k+1}^t = \sigma_k + \mathbb{C} \Delta \varepsilon_{k+1}, \quad \Delta \varepsilon_{k+1} = \varepsilon_{k+1} - \varepsilon_k. \quad (22)$$

By (14)–(22), we can formulate the time discretized elastoplastic constitutive problem as follows. Given the values σ_k , κ_k , ε_k of the stress, the isotropic hardening and the strain, respectively, at the time t_k and given the incremental strain $\Delta \varepsilon_{k+1}$ for the interval $[t_k, t_{k+1}]$, solve the following system of algebraic equations

$$\mathbb{C}^{-1}(\sigma_{k+1}^t - \sigma_{k+1}) = \Delta \gamma_{k+1} \sqrt{\frac{3}{2}} \frac{\text{dev}(\sigma_{k+1})}{\|\text{dev}(\sigma_{k+1})\|_F} \quad (23)$$

$$\kappa_{k+1} - \kappa_k = \Delta \gamma_{k+1} \quad (24)$$

for the unknowns σ_{k+1} , κ_{k+1} , and $\Delta \gamma_{k+1}$, subject to the constraints

$$\Delta \gamma_{k+1} \geq 0, \quad \Phi(\sigma_{k+1}, \kappa_{k+1}) \leq 0, \quad \Delta \gamma_{k+1} \Phi(\sigma_{k+1}, \kappa_{k+1}) = 0. \quad (25)$$

This constitutive problem can be solved explicitly by the return mapping concept (see e.g. [Bl99, NPO08]). It means that we firstly apply the elastic predictor, i.e. we verify whether $\Phi(\sigma_{k+1}^t, \kappa_k) \leq 0$. If it holds then

$$\Delta \gamma_{k+1} = 0, \quad \sigma_{k+1} = \sigma_{k+1}^t. \quad (26)$$

If $\Phi(\sigma_{k+1}^t, \kappa_k) > 0$, then by the plastic corrector we have

$$\Delta \gamma_{k+1} = \frac{1}{3\mu + H_m} \Phi(\sigma_{k+1}^t, \kappa_k), \quad \sigma_{k+1} = \sigma_{k+1}^t - \frac{3\mu}{3\mu + H_m} \sqrt{\frac{2}{3}} \hat{n}(\sigma_{k+1}^t), \quad (27)$$

where

$$\hat{n}(\tau) = \frac{\text{dev}(\tau)}{\|\text{dev}(\tau)\|_F}, \quad \tau \in S. \quad (28)$$

Notice that the second formula in (27) is correctly defined since the denominator $\|\text{dev}(\sigma_{k+1}^t)\|_F > 0$ for $\Phi(\sigma_{k+1}^t, \kappa_k) > 0$. Let us define the stress and hardening operators $T_\sigma(\tau, \omega; \cdot) : S \rightarrow S$, $T_\kappa(\tau, \omega; \cdot) : S \rightarrow S$ with respect to parameters $\tau \in S$, $\omega \in \mathbb{R}_+$, such that for $\eta \in S$

$$T_\sigma(\tau, \omega; \eta) := \mathbb{C}\eta - \frac{3\mu}{3\mu + H_m} \sqrt{\frac{2}{3}} \Phi^+(\tau + \mathbb{C}\eta, \omega) \hat{n}(\tau + \mathbb{C}\eta), \quad (29)$$

$$T_\kappa(\tau, \omega; \eta) := \frac{1}{3\mu + H_m} \Phi^+(\tau + \mathbb{C}\eta, \omega), \quad (30)$$

respectively, where Φ^+ denotes the positive part of the function Φ . Then by (22), (24), (26), (27), (29) and (30),

$$\Delta\kappa_{k+1} = T_\kappa(\sigma_k, \kappa_k; \Delta\varepsilon_{k+1}), \quad \Delta\sigma_{k+1} = T_\sigma(\sigma_k, \kappa_k; \Delta\varepsilon_{k+1}). \quad (31)$$

For the sake of brevity, we will denote the stress operator $T_\sigma(\sigma_k, \kappa_k; \cdot)$ with respect to the current parameters σ_k and κ_k by $T_k(\cdot)$. By [Bl99, GV09, Sy09], the operator $T_k : S \rightarrow S$ is potential, Lipschitz continuous, strongly monotone, and strongly semismooth on S .

Let us note that semismoothness was originally introduced by Mifflin [Mi77] for functionals. Qi and J. Sun [QS93] extended the definition of semismoothness to vector-valued function to investigate the superlinear convergence of the Newton method. The strong semismoothness of the Lipschitz continuous function $T_k(\cdot)$ means that $T_k(\cdot)$ is directionally differentiable on S and has a quadratic approximate property at any $\eta \in S$, i.e. for any $\xi \in S$, $\xi \rightarrow 0$, and any $T_k^o(\eta + \xi) \in \partial T_k(\eta + \xi)$,

$$T_k(\eta + \xi) - T_k(\eta) - T_k^o(\eta + \xi)\xi = O(\|\xi\|_F^2). \quad (32)$$

Here $\partial T_k(\eta + \xi)$ denotes the set of the Clark generalized derivatives of T_k at $\eta + \xi$. Here we will choose the Clark generalized derivative T_k^o of T_k in the following way:

1. If $\Phi(\sigma_k + \mathbb{C}\eta, \kappa_k) \leq 0$, then

$$T_k^o(\eta) = \mathbb{C}. \quad (33)$$

2. If $\Phi(\sigma_k + \mathbb{C}\eta, \kappa_k) > 0$, then

$$\begin{aligned} T_k^o(\eta) &= \mathbb{C} - \frac{3\mu}{3\mu + H_m} \sqrt{\frac{2}{3}} \frac{\partial \Phi(\sigma_k + \mathbb{C}\eta, \kappa_k)}{\partial \eta} \hat{n}(\sigma_k + \mathbb{C}\eta) - \\ &\quad - \frac{3\mu}{3\mu + H_m} \sqrt{\frac{2}{3}} \Phi(\sigma_k + \mathbb{C}\eta, \kappa_k) \frac{\partial \hat{n}(\sigma_k + \mathbb{C}\eta)}{\partial \eta}, \end{aligned} \quad (34)$$

where

$$\begin{aligned} \frac{\partial \Phi(\sigma_k + \mathbb{C}\eta, \kappa_k)}{\partial \eta} &= 2\mu \sqrt{\frac{3}{2}} \hat{n}(\sigma_k + \mathbb{C}\eta), \\ \frac{\partial \hat{n}(\sigma_k + \mathbb{C}\eta)}{\partial \eta} &= 2\mu \frac{\mathbb{I}_d - \hat{n}(\sigma_k + \mathbb{C}\eta) \otimes \hat{n}(\sigma_k + \mathbb{C}\eta)}{\|\text{dev}(\sigma_k + \mathbb{C}\eta)\|_F}, \\ \mathbb{I}_d \xi &:= \text{dev}(\xi), \quad \forall \xi \in S. \end{aligned}$$

Notice that T_k is not differentiable at $\eta \in S$, $\Phi(\sigma_k + \mathbb{C}\eta, \kappa_k) = 0$. Otherwise $T_k^o(\eta) = \partial T_k(\eta) / \partial \eta$.

Let us recall that the stress, strain, hardening and displacement variables also depend on a spatial variable $x \in \Omega$. We consider the dependence of $T_k(\Delta\varepsilon_k)$ on x in the following sense:

$$T_k(\Delta\varepsilon_k) = T_k(\Delta\varepsilon_k)(x) := T_\sigma(\sigma_k(x), \kappa_k(x); \Delta\varepsilon_k(x)). \quad (35)$$

Then we can substitute the stress operator T_k , defined by (29), into the balance equation (6) to obtain the time discretized elastoplastic problem in the incremental form.

Problem 2 (One time step elastoplastic problem in the incremental form). Given the stress field $\sigma_k \in [L^2(\Omega)]_{sym}^{3 \times 3}$ and the isotropic hardening field $\kappa_k \in L^2(\Omega)$ at the time t_k , find the displacement $u_{k+1} = u_k + \Delta u_{k+1} \in V$, where the increment $\Delta u_{k+1} \in V$ solves the variational equation

$$\int_{\Omega} \langle T_k(\varepsilon(\Delta u_{k+1})), \varepsilon(v) \rangle_F dx = \int_{\Omega} \Delta g_{k+1}^T v dx + \int_{\Gamma_N} \Delta F_{k+1}^T v ds \quad \forall v \in V, \quad (36)$$

with loading increments $\Delta F_{k+1} = F_{k+1} - F_k$, $\Delta g_{k+1} = g_{k+1} - g_k$. Set the stress and isotropic hardening fields $\sigma_{k+1} = \sigma_k + \Delta \sigma_{k+1}$, $\kappa_{k+1} = \kappa_k + \Delta \kappa_{k+1}$ in the next time step t_{k+1} from the relations

$$\Delta \sigma_{k+1} = T_{\sigma}(\sigma_k, \kappa_k; \varepsilon(\Delta u_{k+1})), \quad \Delta \kappa_{k+1} = T_{\kappa}(\sigma_k, \kappa_k; \varepsilon(\Delta u_{k+1})), \quad (37)$$

almost everywhere in Ω .

Problem 2 can be equivalently formulated as a minimization problem [GV09, Sy09]. Since the operator T_k is strongly monotone and Lipschitz continuous on S , the non-linear equation (36) has a unique solution $\Delta u_{k+1} \in V$ (see e.g. [FK80]). As we will see in the next section, we will solve a linearized problem in each Newton iteration. To do this, it will be useful to define the bilinear form $a_k(u) : V \times V \rightarrow \mathbb{R}$ for $u \in V$ by

$$a_k(u)(w, v) = \int_{\Omega} \langle T_k^o(\varepsilon(u))\varepsilon(w), \varepsilon(v) \rangle dx, \quad v, w \in V, \quad (38)$$

where the operator $T_k^o(\cdot) = T_k^o(\cdot)(x)$ is defined by (33) and (34). Since the operator T_k is potential, Lipschitz continuous and strongly monotone on S , the bilinear form a_k is symmetric and V -elliptic on V .

3 Semismooth Newton method in elastoplasticity

In this section, firstly, we approximate the time discretized elastoplastic problem by the finite element method and introduce the corresponding algebraic notation. Secondly, we introduce the semismooth Newton method for the problem.

3.1 Finite element discretization and algebraic formulation

Details to finite element implementation of elastoplastic problems can be found in [CK02] and [Bl99, GV09].

For the sake of simplicity, we assume a polynomial 3D domain Ω and use the linear simplex elements. The corresponding shape regular triangulation is denoted by \mathcal{T}_h . Thus the space V is approximated by its subspace V_h of piecewise linear and continuous functions. Therefore the spaces of the strains, the stress and the isotropic hardening are approximated by piecewise constant functions.

Similarly to (36), (37), we can formulate the one time step elastoplastic problem after the space discretization. Let $\sigma_{k,h}$, $\kappa_{k,h}$, $u_{k,h}$ be piecewise constant stress and hardening variables with respect to the triangulation \mathcal{T}_h at the time t_k obtained from a previous time process.

Problem 3 (One time step elastoplastic problem in the incremental form after space discretization). Find the displacement $u_{k+1,h} = u_{k,h} + \Delta u_{k+1,h} \in V_h$, where the increment $\Delta u_{k+1,h} \in V_h$ solves the variational equation

$$\int_{\Omega} \langle T_{k,h}(\varepsilon(\Delta u_{k+1,h})), \varepsilon(v_h) \rangle_F dx = \int_{\Omega} \Delta g_{k+1}^T v_h dx + \int_{\Gamma_N} \Delta F_{k+1}^T v_h ds \quad \forall v_h \in V_h, \quad (39)$$

where $T_{k,h}(\cdot) := T_{\sigma}(\sigma_{k,h}, \kappa_{k,h}; \cdot)$. Set the stress and isotropic hardening fields $\sigma_{k+1,h} = \sigma_{k,h} + \Delta \sigma_{k+1,h}$, $\kappa_{k+1,h} = \kappa_{k,h} + \Delta \kappa_{k+1,h}$ in the next time step t_{k+1} from the relations

$$\Delta \sigma_{k+1,h} = T_{\sigma}(\sigma_{k,h}, \kappa_{k,h}; \varepsilon(\Delta u_{k+1,h})), \quad \Delta \kappa_{k+1,h} = T_{\kappa}(\sigma_{k,h}, \kappa_{k,h}; \varepsilon(\Delta u_{k+1,h})) \quad (40)$$

for every elements of \mathcal{T}_h .

For the sake of simplicity, we do not consider finite element approximation of F_k and g_k . Similarly as in (33) and (34), we can define the generalized derivative $T_{k,h}^o$ of $T_{k,h}$ and consequently also define the approximated bilinear form $a_{k,h}(u_h)$ for $u_h \in V_h$ by

$$a_{k,h}(u_h)(w_h, v_h) = \int_{\Omega} \langle T_{k,h}^o(\varepsilon(u_h))\varepsilon(w_h), \varepsilon(v_h) \rangle dx, \quad v_h, w_h \in V_h. \quad (41)$$

Each function $v_h = (v_{h,1}, v_{h,2}, v_{h,3}) \in V_h$ can be represented by a vector

$$\mathbf{v} \in \mathbb{R}^n, \quad \mathbf{v} := (v_{h,j}(x_i))_{i \in \{1, \dots, \mathcal{N}\}, j \in \{1, 2, 3\}},$$

where \mathcal{N} denotes the number of vertices of the triangulation \mathcal{T}_h and $n = 3\mathcal{N}$. The homogeneous Dirichlet boundary condition is represented by a restriction matrix $\mathbf{B}_U \in \mathbb{R}^{m \times n}$, i.e.

$$\mathbf{B}_U \mathbf{u} = \mathbf{o}. \quad (42)$$

Let $\mathbf{R}_T \in \mathbb{R}^{12 \times n}$ be a restriction operator for a displacement vector $\mathbf{u} \in \mathbb{R}^n$ on a local element $T \in \mathcal{T}_h$, i.e.

$$\mathbf{u}_T = \mathbf{R}_T \mathbf{u}. \quad (43)$$

We denote by \mathbf{u}_k and $\Delta \mathbf{u}_{k+1}$ the displacement vector and the searching displacement increment at the time step k , respectively. We denote the load vector represented the volume and surface forces F_k, g_k by \mathbf{f}_k and its increment $\Delta \mathbf{f}_k$.

Further, we use a vector representation in \mathbb{R}^6 of the stress and strain tensors that is typical for an implementation of elastic problem, i.e.

$$\boldsymbol{\sigma} = (\sigma_{11}, \sigma_{22}, \sigma_{33}, \sigma_{12}, \sigma_{23}, \sigma_{13})^T, \quad \boldsymbol{\varepsilon} = (\varepsilon_{11}, \varepsilon_{22}, \varepsilon_{33}, 2\varepsilon_{12}, 2\varepsilon_{23}, 2\varepsilon_{13})^T. \quad (44)$$

Notice that the stress and strain vectors have different structures in comparison to the above tensor notation. Therefore we must carefully distinguish this difference in algebraic representation of the operators $T_\sigma, T_\kappa, T_{k,h}$, and $T_{k,h}^o$. The vectors in sense of stress variables will be denoted by letters $\boldsymbol{\sigma}, \boldsymbol{\tau}$, the vectors in sense of strain variables will be denoted by letters $\boldsymbol{\varepsilon}, \boldsymbol{\varepsilon}^p, \boldsymbol{\eta}$, and $\boldsymbol{\xi}$. Let $\boldsymbol{\sigma}_{k,T}$ and $\boldsymbol{\kappa}_{k,T}$ be the algebraic representation of $\sigma_{k,h}$ and $\kappa_{k,h}$ on an element $T \in \mathcal{T}_h$, respectively.

We introduce the algebraic representations $\mathbf{C} \in \mathbb{R}^{6 \times 6}$, $\mathbf{E}_\varepsilon \in \mathbb{R}^{6 \times 6}$, $\mathbf{E}_\sigma \in \mathbb{R}^{6 \times 6}$, $\|\cdot\|_\sigma$, Φ , $\hat{\mathbf{n}}, \mathbf{T}_{\kappa,k,T}, \mathbf{T}_{k,T}$, and $\mathbf{T}_{k,T}^o$ of the Hooke tensor \mathbb{C} , the deviatoric operator \mathbb{I}_d related to the strain and stress variables, the Frobenius norm with respect to a stress variable, the functions Φ , $\hat{\mathbf{n}}$, and the restrictions of the functions $T_\kappa(\sigma_k|_T, \kappa_k|_T, \cdot)$, $T_{k,h}$, $T_{k,h}^o$ on $T \in \mathcal{T}_h$, respectively, with respect to the vector form (44) of the stress and strain variables. The forms of matrices \mathbf{C} , \mathbf{E}_ε , \mathbf{E}_σ , and the norm $\|\cdot\|_\sigma$ are

$$\begin{aligned} \mathbf{C} &:= \begin{bmatrix} \lambda + 2\mu & \lambda & \lambda & 0 & 0 & 0 \\ \lambda & \lambda + 2\mu & \lambda & 0 & 0 & 0 \\ \lambda & \lambda & \lambda + 2\mu & 0 & 0 & 0 \\ 0 & 0 & 0 & \mu & 0 & 0 \\ 0 & 0 & 0 & 0 & \mu & 0 \\ 0 & 0 & 0 & 0 & 0 & \mu \end{bmatrix}, \\ \mathbf{E}_\varepsilon &:= \frac{1}{3} \begin{bmatrix} 2 & -1 & -1 & 0 & 0 & 0 \\ -1 & 2 & -1 & 0 & 0 & 0 \\ -1 & -1 & 2 & 0 & 0 & 0 \\ 0 & 0 & 0 & 1.5 & 0 & 0 \\ 0 & 0 & 0 & 0 & 1.5 & 0 \\ 0 & 0 & 0 & 0 & 0 & 1.5 \end{bmatrix}, \\ \mathbf{E}_\sigma &:= \mathbf{P} \mathbf{E}_\varepsilon, \quad \mathbf{P} := \text{diag}(1, 1, 1, 2, 2, 2), \end{aligned}$$

and

$$\|\boldsymbol{\tau}\|_\sigma := (\boldsymbol{\tau}^T \mathbf{P} \boldsymbol{\tau})^{1/2}, \quad \boldsymbol{\tau} \in \mathbb{R}^6,$$

respectively. Consequently the functions Φ , $\hat{\mathbf{n}}, \mathbf{T}_{\kappa,k,T}, \mathbf{T}_{k,T}, \mathbf{T}_{k,T}^o$ are defined by (16), (28), (30), (29), (33), (34) in the following way:

$$\begin{aligned} \Phi(\boldsymbol{\tau}, \boldsymbol{\kappa}) &:= \sqrt{\frac{3}{2}} \|\mathbf{E}_\sigma \boldsymbol{\tau}\|_\sigma - (\sigma_y + H_m \boldsymbol{\kappa}), \\ \hat{\mathbf{n}}(\boldsymbol{\tau}) &:= \frac{\mathbf{E}_\sigma(\boldsymbol{\tau})}{\|\mathbf{E}_\sigma(\boldsymbol{\tau})\|_\sigma}, \quad \bar{\mathbf{n}}_{k,T}(\boldsymbol{\eta}) = \hat{\mathbf{n}}(\boldsymbol{\sigma}_{k,T} + \mathbf{C}\boldsymbol{\eta}), \\ \mathbf{T}_{\kappa,k,T}(\boldsymbol{\eta}) &:= \frac{1}{3\mu + H_m} \Phi^+(\boldsymbol{\sigma}_{k,T} + \mathbf{C}\boldsymbol{\eta}, \boldsymbol{\kappa}_{k,T}), \end{aligned}$$

$$\mathbf{T}_{k,T}(\boldsymbol{\eta}) := \mathbf{C}\boldsymbol{\eta} - \frac{3\mu}{3\mu + H_m} \sqrt{\frac{2}{3}} \boldsymbol{\Phi}^+ (\boldsymbol{\sigma}_{k,T} + \mathbf{C}\boldsymbol{\eta}, \boldsymbol{\kappa}_{k,T}) \bar{\mathbf{n}}_{k,T}(\boldsymbol{\eta}),$$

$$\mathbf{T}_{k,T}^o(\boldsymbol{\eta}) := \begin{cases} \mathbf{C}, & \text{if } \boldsymbol{\Phi}(\boldsymbol{\sigma}_{k,T} + \mathbf{C}\boldsymbol{\eta}, \boldsymbol{\kappa}_{k,T}) \leq 0, \text{ otherwise} \\ \mathbf{C} - 2\mu \frac{3\mu}{3\mu + H_m} \mathbf{E}_\varepsilon - \\ - 2\mu \frac{3\mu}{3\mu + H_m} \sqrt{\frac{2}{3}} \frac{\sigma_y + H_m \boldsymbol{\kappa}_{k,T}}{\|\mathbf{E}_\sigma(\boldsymbol{\sigma}_{k,T} + \mathbf{C}\boldsymbol{\eta})\|_\sigma} \left(\bar{\mathbf{n}}_{k,T}(\boldsymbol{\eta}) \bar{\mathbf{n}}_{k,T}^T(\boldsymbol{\eta}) - \mathbf{E}_\varepsilon \right), \end{cases}$$

respectively.

We also introduce the matrix $\mathbf{G} \in \mathbb{R}^{6 \times 12}$ representing the algebraical relation between the strain and the displacement (the exact form of \mathbf{G} is in [ACFK02]), i.e. the strain $\boldsymbol{\varepsilon}_T$ on an element $T \in \mathcal{T}_h$ can be found by (43) in the form

$$\boldsymbol{\varepsilon}_T = \mathbf{G}\mathbf{R}_T \mathbf{u}. \quad (45)$$

Based on the introduced notation we define the non-linear operator $\mathbf{F}_k : \mathbb{R}^n \rightarrow \mathbb{R}^n$,

$$\mathbf{F}_k(\mathbf{v}) = \sum_{T \in \mathcal{T}_h} (\mathbf{T}_{k,T}(\mathbf{G}\mathbf{R}_T \mathbf{v}))^T \mathbf{G}\mathbf{R}_T, \quad \mathbf{v} \in \mathbb{R}^n, \quad (46)$$

which represents the left hand side in (39), and the stiffness matrix $\mathbf{K}_k(\mathbf{v}) \in \mathbb{R}^{n \times n}$, $\mathbf{v} \in \mathbb{R}^n$,

$$\mathbf{K}_k(\mathbf{v}) = \sum_{T \in \mathcal{T}_h} (\mathbf{T}_{k,T}^o(\mathbf{G}\mathbf{R}_T \mathbf{v}) \mathbf{G}\mathbf{R}_T)^T \mathbf{G}\mathbf{R}_T, \quad (47)$$

which represents the bilinear form $a_{k,h}(v_h)$. In particular, we denote the matrix $\mathbf{K}_k(\Delta \mathbf{u}_{k+1,i})$ briefly by $\mathbf{K}_{k,i}$, where the reason of $\Delta \mathbf{u}_{k+1,i} \in \mathbb{R}^n$ will be explained in the next section.

Let

$$\mathbf{V} := \{\mathbf{v} \in \mathbb{R}^n \mid \mathbf{B}_U \mathbf{v} = \mathbf{o}\}.$$

Then by using (46), we can rewrite the equation (39) as follows: find $\Delta \mathbf{u}_{k+1} \in \mathbf{V}$ such that

$$\mathbf{v}^T (\mathbf{F}_k(\Delta \mathbf{u}_{k+1}) - \Delta \mathbf{f}_{k+1}) = 0 \quad \forall \mathbf{v} \in \mathbf{V}, \quad (48)$$

where $\Delta \mathbf{f}_{k+1}$ is the increment of the load vector. Let $\tilde{\mathbf{u}}_k \in \mathbb{R}^{n-m}$, $\tilde{\mathbf{f}}_k \in \mathbb{R}^{n-m}$, $\tilde{\mathbf{K}}_{k,i} \in \mathbb{R}^{(n-m) \times (n-m)}$, and $\tilde{\mathbf{F}}_k : \mathbb{R}^{n-m} \rightarrow \mathbb{R}^{n-m}$ denote the restrictions of \mathbf{u}_k , \mathbf{f}_k , $\mathbf{K}_{k,i}$, and \mathbf{F}_k given by omitting the entries (degrees of freedom) corresponding to the prescribed Dirichlet boundary conditions. Then we can rewrite the equation (48) to the following system of non-linear equations:

$$\text{find } \Delta \mathbf{u}_{k+1} \in \mathbf{V} : \quad \tilde{\mathbf{F}}_k(\Delta \tilde{\mathbf{u}}_{k+1}) = \Delta \tilde{\mathbf{f}}_{k+1}. \quad (49)$$

The discretized elastoplastic problem can be solved by the following algorithm:

Algorithm 1 (Solution of discretized elastoplastic problem).

- 1: initial step: $\mathbf{u}_0 = \mathbf{o}$, $\boldsymbol{\varepsilon}_{0,T} = \mathbf{o}$, $\boldsymbol{\sigma}_{0,T} = \mathbf{o}$, $\boldsymbol{\kappa}_{0,T} = \mathbf{o}$ for any $T \in \mathcal{T}_h$
- 2: **for** $k = 0, \dots, N - 1$ **do**
- 3: find $\Delta \mathbf{u}_{k+1} \in \mathbf{V} : \tilde{\mathbf{F}}_k(\Delta \tilde{\mathbf{u}}_{k+1}) = \Delta \tilde{\mathbf{f}}_{k+1}$
- 4: **for all** $T \in \mathcal{T}_h$ **do**
- 5: $\Delta \boldsymbol{\varepsilon}_{k+1,T} = \mathbf{G}\mathbf{R}_T \Delta \mathbf{u}_{k+1}$, $\boldsymbol{\varepsilon}_{k+1,T} = \boldsymbol{\varepsilon}_{k,T} + \Delta \boldsymbol{\varepsilon}_{k+1,T}$
- 6: $\Delta \boldsymbol{\sigma}_{k+1,T} = \mathbf{T}_{k,T}(\Delta \boldsymbol{\varepsilon}_{k+1,T})$, $\boldsymbol{\sigma}_{k+1,T} = \boldsymbol{\sigma}_{k,T} + \Delta \boldsymbol{\sigma}_{k+1,T}$
- 7: $\Delta \boldsymbol{\kappa}_{k+1,T} = \mathbf{T}_{\kappa,k,T}(\Delta \boldsymbol{\varepsilon}_{k+1,T})$, $\boldsymbol{\kappa}_{k+1,T} = \boldsymbol{\kappa}_{k,T} + \Delta \boldsymbol{\kappa}_{k+1,T}$
- 8: **end for**
- 9: **end for**

3.2 Semismooth Newton method for one time step problem

The non-linear system of equations (49) is solved by the semismooth Newton method (see e.g. [QS93]). The corresponding algorithm is following:

Algorithm 2 (Semismooth Newton method).

- 1: initialization: $\Delta \mathbf{u}_{k,0} = \mathbf{o}$
- 2: **for** $i = 0, 1, 2, \dots$ **do**
- 3: find $\delta \mathbf{u}_i \in \mathbf{V}$: $\tilde{\mathbf{K}}_{k,i} \delta \tilde{\mathbf{u}}_i = \Delta \tilde{\mathbf{f}}_{k+1} - \tilde{\mathbf{F}}_k(\Delta \tilde{\mathbf{u}}_{k,i})$
- 4: compute $\Delta \mathbf{u}_{k,i+1} = \Delta \mathbf{u}_{k,i} + \delta \mathbf{u}_i$
- 5: **if** $\|\Delta \mathbf{u}_{k,i+1} - \Delta \mathbf{u}_{k,i}\| / (\|\Delta \mathbf{u}_{k,i+1}\| + \|\Delta \mathbf{u}_{k,i}\|) \leq \epsilon_{Newton}$ **then stop**
- 6: **end for**
- 7: set $\Delta \mathbf{u}_{k+1} = \Delta \mathbf{u}_{k,i+1}$

Here $\epsilon_{Newton} > 0$ is the relative stopping tolerance and $\delta \tilde{\mathbf{u}}_i \in \mathbb{R}^{n-m}$ is the restriction of $\delta \mathbf{u}_i$ given by omitting the entries (degrees of freedom) corresponding to the prescribed Dirichlet boundary conditions. The systems of linear equations, which are considered in each Newton iteration, will be solved by the TFETI method introduced in the next section.

In [Bl99, GV09, Sy09], superlinear local convergence of the algorithm has been derived. Let us note that the convergence depends on the discretization parameter h of the triangulation. Therefore we can expect that the finer mesh the bigger number of the Newton iterations. In [Sy09], a damped semismooth Newton method for such a problem has also been described. Such a method has again superlinear local convergence and additionally global convergence.

4 TFETI method for solving linearized problems

In this section, we describe the TFETI domain decomposition method for solving linearized problems appearing in Newton iterations and its optimal solver based on projected conjugate gradient method with a lumped preconditioner. Finally, we summarize TFETI based algorithm for solving the whole elastoplastic problem.

4.1 TFETI domain decomposition method

In the previous section, we showed that we need to solve the following system of the linear equations:

$$\text{find } \delta \mathbf{u}_i \in \mathbf{V} : \quad \tilde{\mathbf{K}}_{k,i} \delta \tilde{\mathbf{u}}_i = \Delta \tilde{\mathbf{f}}_{k+1} - \tilde{\mathbf{F}}_k(\Delta \tilde{\mathbf{u}}_{k,i}) \quad (50)$$

in each time step k and in each Newton iteration i . Since the TFETI domain decomposition method can be described independently of the indices k, i , we will schematically write the problem in the form:

$$\text{find } \mathbf{u} \in \mathbf{V} : \quad \tilde{\mathbf{K}} \tilde{\mathbf{u}} = \tilde{\mathbf{f}}, \quad (51)$$

where $\tilde{\mathbf{K}}, \tilde{\mathbf{u}}, \tilde{\mathbf{f}}$ are the restriction of $\mathbf{K}, \mathbf{u}, \mathbf{f}$ with respect to the Dirichlet boundary conditions respectively. Let us note that \mathbf{K} is a symmetric and positive semidefinite matrix and $\tilde{\mathbf{K}}$ is a symmetric and positive definite matrix. Therefore the linearized problem (51) has a unique solution. The problem (51) can be equivalently rewritten as a minimum problem:

$$\text{find } \mathbf{u} \in \mathbf{V} : \quad \mathbf{J}(\mathbf{u}) \leq \mathbf{J}(\mathbf{v}), \quad \forall \mathbf{v} \in \mathbf{V}, \quad (52)$$

where

$$\mathbf{J}(\mathbf{v}) = \frac{1}{2} \mathbf{v}^T \mathbf{K} \mathbf{v} - \mathbf{f}^T \mathbf{v}, \quad \mathbf{v} \in \mathbf{V}.$$

The corresponding functional representation of (51) is following: find $u_h \in V_h$ such that for any $v_h \in V_h$,

$$\int_{\Omega} \langle \mathbb{D}_h \varepsilon(u_h), \varepsilon(v_h) \rangle_F dx = \int_{\Omega} g^T v_h dx + \int_{\Gamma_N} F^T v_h ds - \int_{\Omega} \langle \tau_h, \varepsilon(v_h) \rangle_F dx, \quad (53)$$

where \mathbb{D}_h restricted on $T \in \mathcal{T}_h$ is a constant fourth order symmetric and elliptic tensor and τ_h restricted on $T \in \mathcal{T}_h$ is a constant second order tensor from S . We can see that (53) is related to (50), if we replace

$$\mathbb{D}_h \sim T_{k,h}^o(\Delta u_{k,h,i}), \quad \tau_h \sim T_{k,h}(\Delta u_{k,h,i}), \quad F \sim \Delta F_{k+1}, \quad g \sim \Delta g_{k+1}, \quad u_h \sim \delta u_{h,i}$$

and set $\Delta u_{k,h,i}$ and $\delta u_{h,i}$ as the functional representation of $\Delta \mathbf{u}_{k,i}$ and $\delta \mathbf{u}_i$, respectively.

Notice that the problem (53) has a similar scheme as the elastic problem defined in Subsection 2.2. Therefore the below introduced TFETI method can also be explained for elasticity in the same way.

The variational problem of the type (53) can be equivalently formulated as a minimization problem:

$$\text{find } u_h \in V_h : \quad J_h(u_h) \leq J_h(v_h) \quad \forall v_h \in V_h, \quad (54)$$

where

$$J_h(v_h) = \frac{1}{2} \int_{\Omega} \langle \mathbb{D}_h \varepsilon(v_h), \varepsilon(v_h) \rangle_F dx - \int_{\Omega} g^T v_h dx - \int_{\Gamma_N} F^T v_h ds + \int_{\Omega} \langle \tau_h, \varepsilon(v_h) \rangle_F dx. \quad (55)$$

To apply the TFETI domain decomposition, we tear the body from the part of the boundary with the Dirichlet boundary condition, decompose it into subdomains, assign each subdomain by a unique number, and introduce new ‘‘gluing’’ conditions on the artificial intersubdomain boundaries and on the boundaries with imposed Dirichlet condition (see Figure 2).

In particular, the polynomial domain Ω is decomposed into a system of s disjoint polynomial subdomains $\Omega^p \subset \mathbb{R}^3$, $p = 1, 2, \dots, s$. We assume that the decomposition is consistent with the triangulation \mathcal{T}_h , i.e.

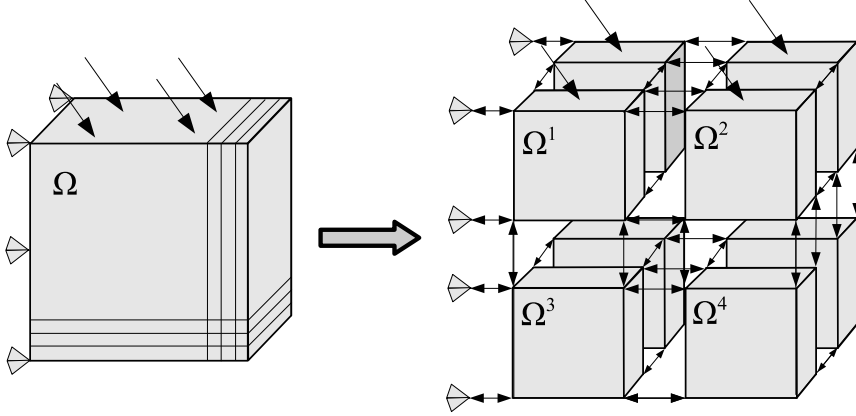


Figure 2: TFETI domain decomposition with subdomain renumbering

$$\forall T \in \mathcal{T}_h \exists! p \in \{1, 2, \dots, s\} : \quad T \subset \bar{\Omega}^p \quad (56)$$

and define

$$\mathcal{T}_h^p := \{T \in \mathcal{T}_h : T \subset \bar{\Omega}^p\}, \quad \mathcal{T}_h = \bigcup_{p \in \{1, 2, \dots, s\}} \mathcal{T}_h^p. \quad (57)$$

After the decomposition each boundary Γ^p of Ω^p consists of three disjoint parts Γ_U^p , Γ_N^p , and Γ_G^p , $\Gamma^p = \bar{\Gamma}_U^p \cup \bar{\Gamma}_N^p \cup \bar{\Gamma}_G^p$, where

$$\Gamma_U^p = \Gamma_U \cap \Gamma^p, \quad \Gamma_N^p = \Gamma_N \cap \Gamma^p, \quad \Gamma_G^p = \bigcup_{q \in \{1, 2, \dots, s\} \setminus \{p\}} \Gamma_G^{pq},$$

with Γ_G^{pq} being the part of Γ^p which is glued to Ω^q , $p \neq q$.

Similarly to the definition of V_h , we can define the spaces V_h^p , $p = 1, 2, \dots, s$, of piecewise linear and continuous approximations of $H^1(\Omega^p)$:

$$V_h^p := \{v_h^p \in H^1(\Omega^p) : v_h^p|_T \in [P_1]^3 \quad \forall T \in \mathcal{T}_h^p, \quad v_h^p|_{\Gamma_U^p} = 0\}. \quad (58)$$

Let $\mathbf{V}_h := V_h^1 \times V_h^2 \times \dots \times V_h^s$ be a product space and

$$\mathbf{K}_h := \{\mathbf{v}_h = (v_h^1, \dots, v_h^s) \in \mathbf{V}_h : v_h^p = v_h^q \text{ on } \Gamma_G^{pq} \quad \forall p, q \in \{1, 2, \dots, s\}, p \neq q\}. \quad (59)$$

Let us note that we slightly distinguish the notation introduced for the TFETI method from the notation introduced in Sections 2 and 3. For example, we write \mathbf{V}_h for the TFETI method while in Section 2, we used the notation V_h . A similar distinction is also introduced for the below algebraic description of the TFETI method.

Let

$$\begin{aligned} \mathbf{J}_h(\mathbf{v}_h) = & \sum_{p=1}^s \left\{ \frac{1}{2} \int_{\Omega^p} \langle \mathbb{D}_h \varepsilon(v_h^p), \varepsilon(v_h^p) \rangle_F dx - \int_{\Omega^p} g^T v_h^p dx \right. \\ & \left. - \int_{\Gamma_N^p} F^T v_h^p ds + \int_{\Omega^p} \langle \tau_h, \varepsilon(v_h^p) \rangle_F dx \right\} \end{aligned} \quad (60)$$

be a functional defined on \mathbf{V}_h . Then the minimization problem (54) can be equivalently rewritten into the form:

$$\text{find } \mathbf{u}_h \in \mathbf{K}_h : \quad \mathbf{J}_h(\mathbf{u}_h) \leq \mathbf{J}_h(\mathbf{v}_h) \quad \forall \mathbf{v}_h \in \mathbf{K}_h, \quad (61)$$

where $\mathbf{u}_h = ((u_h)|_{\Omega^1}, \dots, (u_h)|_{\Omega^s})$ and $u_h \in V_h$ solves (54).

Each function $\mathbf{v}_h = (v_h^1, v_h^2, \dots, v_h^s)$, $\mathbf{v}_h \in \mathbf{V}_h$, can be represented by a vector $\mathbf{v} \in \mathbb{R}^n$, $\mathbf{v} = (\mathbf{v}_1^T, \mathbf{v}_2^T, \dots, \mathbf{v}_s^T)^T$, where $\mathbf{v}_p \in \mathbb{R}^{n_p}$, $p \in \{1, 2, \dots, s\}$, is the algebraic representation of v_h^p and $n = \sum_{p=1}^s n_p$. Similarly we can find the vector $\mathbf{f} \in \mathbb{R}^n$, $\mathbf{f} = (\mathbf{f}_1^T, \mathbf{f}_2^T, \dots, \mathbf{f}_s^T)^T$, $\mathbf{f}_p \in \mathbb{R}^{n_p}$, $p \in \{1, 2, \dots, s\}$, such that \mathbf{f}_p is the algebraic representation of the load restricted on Ω^p and Γ_N^p . Let the matrix $\mathbf{B}_G \in \mathbb{R}^{m_G \times n}$ represent the gluing conditions introduced in (59) and $\mathbf{B}_U \in \mathbb{R}^{m_U \times n}$ the Dirichlet boundary conditions introduced in (58). More details about matrices \mathbf{B}_G and \mathbf{B}_U can be found in [KVMHDKC12]. Both matrices can be combined into one constraint matrix

$$\mathbf{B} = \begin{bmatrix} \mathbf{B}_G \\ \mathbf{B}_U \end{bmatrix}, \quad \mathbf{B} \in \mathbb{R}^{m \times n}, \quad m = m_G + m_U.$$

Typically m is much smaller than n . Let the matrix $\mathbf{K} \in \mathbb{R}^{n \times n}$, $\mathbf{K} = \text{diag}(\mathbf{K}_1, \mathbf{K}_2, \dots, \mathbf{K}_s)$ denotes a symmetric positive semidefinite block diagonal matrix, where

$$\mathbf{K}_p = \sum_{T \in \mathcal{T}_h^p} |T| (\mathbf{D}_T \mathbf{G} \mathbf{R}_T^p)^T \mathbf{G} \mathbf{R}_T^p, \quad \mathbf{K}_p \in \mathbb{R}^{n_p \times n_p}.$$

Here $\mathbf{D}_T \in \mathbb{R}^{6 \times 6}$ is the algebraic representation of $\mathbb{D}_h|_T$ and $\mathbf{R}_T^p \in \mathbb{R}^{12 \times n_p}$ is a restriction operator for a displacement vector $\mathbf{u}_p \in \mathbb{R}^{n_p}$ to a local element $T \in \mathcal{T}_h^p$. The diagonal blocks \mathbf{K}_p , $p \in \{1, 2, \dots, s\}$, which correspond to the subdomains Ω^p , are positive semidefinite sparse matrices with known kernels, the rigid body modes.

The algebraical formulation of (61) is following:

$$\begin{cases} \text{find } \mathbf{u} \in \mathbf{V} & : \quad \mathbf{J}(\mathbf{u}) \leq \mathbf{J}(\mathbf{v}) \quad \forall \mathbf{v} \in \mathbf{V}, \\ \mathbf{J}(\mathbf{v}) & := \frac{1}{2} \mathbf{v}^T \mathbf{K} \mathbf{v} - \mathbf{f}^T \mathbf{v}, \\ \mathbf{V} & := \{\mathbf{v} \in \mathbb{R}^n : \mathbf{B} \mathbf{v} = \mathbf{o}\}. \end{cases} \quad (62)$$

Even though (62) is a standard convex quadratic programming problem, its formulation is not suitable for numerical solution. The reasons are that \mathbf{K} is typically ill-conditioned, singular, and very large.

The complications mentioned above may be essentially reduced by applying the duality theory of convex programming (see, e.g., Dostál [D09]), where all the constraints are enforced by the Lagrange multipliers $\boldsymbol{\lambda}$. The Lagrangian associated with problem (62) is

$$L(\mathbf{v}, \boldsymbol{\lambda}) = \mathbf{J}(\mathbf{v}) + \boldsymbol{\lambda}^T \mathbf{B} \mathbf{v}. \quad (63)$$

It is well known [D09] that (62) is equivalent to the saddle point problem:

$$\text{find } (\mathbf{u}, \boldsymbol{\lambda}) \in \mathbb{R}^n \times \mathbb{R}^m : \quad L(\mathbf{u}, \boldsymbol{\nu}) \leq L(\mathbf{u}, \boldsymbol{\lambda}) \leq L(\mathbf{v}, \boldsymbol{\lambda}) \quad \forall (\mathbf{v}, \boldsymbol{\nu}) \in \mathbb{R}^n \times \mathbb{R}^m \quad (64)$$

in sense that \mathbf{u} solves (62) if and only if $(\mathbf{u}, \boldsymbol{\lambda})$ solves (64).

4.2 Optimal solvers to equality constrained problems

The solution of (64) leads to the equivalent problem to find $(\mathbf{u}, \boldsymbol{\lambda}) \in \mathbb{R}^{\mathbf{n}} \times \mathbb{R}^{\mathbf{m}}$ satisfying:

$$\begin{pmatrix} \mathbf{K} & \mathbf{B}^T \\ \mathbf{B} & \mathbf{0} \end{pmatrix} \begin{pmatrix} \mathbf{u} \\ \boldsymbol{\lambda} \end{pmatrix} = \begin{pmatrix} \mathbf{f} \\ \mathbf{o} \end{pmatrix}. \quad (65)$$

The system (65) is uniquely solvable which is guaranteed by the following necessary and sufficient conditions [BGL05]:

$$\text{Ker} \mathbf{B}^T = \mathbf{o}, \quad (66)$$

$$\text{Ker} \mathbf{K} \cap \text{Ker} \mathbf{B} = \mathbf{o}. \quad (67)$$

Notice that (66) is the condition on the full row-rank of \mathbf{B} . Let us mention that an orthonormal basis of $\text{Ker} \mathbf{K}$ is known à-priori and that its vectors are columns of $\mathbf{R} \in \mathbb{R}^{\mathbf{n} \times l}$, $l = \mathbf{n} - \text{rank}(\mathbf{K})$.

The first equation in (65) is satisfied if

$$\mathbf{f} - \mathbf{B}^T \boldsymbol{\lambda} \in \text{Im} \mathbf{K} \quad (68)$$

and

$$\mathbf{u} = \mathbf{K}^\dagger (\mathbf{f} - \mathbf{B}^T \boldsymbol{\lambda}) + \mathbf{R} \boldsymbol{\alpha} \quad (69)$$

for an appropriate $\boldsymbol{\alpha} \in \mathbb{R}^l$ and arbitrary matrix \mathbf{K}^\dagger satisfying $\mathbf{K} \mathbf{K}^\dagger \mathbf{K} = \mathbf{K}$. Here \mathbf{K}^\dagger is a generalized inverse matrix whose application on a vector can be efficiently implemented (see Remark 1).

Remark 1. The diagonal block \mathbf{K}_p , $p \in \{1, 2, \dots, s\}$, which corresponds to the subdomain Ω^p , is positive semidefinite sparse matrix with known kernel basis created by the rigid body modes. This is a great advantage because all blocks can be effectively regularized without extra fill in and then decomposed using any standard sparse Cholesky type factorization method for nonsingular matrices [BDKKM10]. We completely avoid problems with zero pivots. The action of \mathbf{K}^\dagger on a vector is naturally parallelized with respect to the subdomains and computed using backward and forward substitutions.

Remark 2. Notice that the pseudoinverse \mathbf{K}^\dagger can also be applied on vectors which do not belong to $\text{Im}(\mathbf{K})$. Therefore we can write $\mathbf{K}^\dagger (\mathbf{f} - \mathbf{B}^T \boldsymbol{\lambda}) = \mathbf{K}^\dagger \mathbf{f} - \mathbf{K}^\dagger (\mathbf{B}^T \boldsymbol{\lambda})$ in the other text. The random error corresponding with this partition is neglected with respect to the implementation of \mathbf{K}^\dagger introduced in Remark 1.

The condition (68) can be equivalently written as

$$\mathbf{R}^T (\mathbf{f} - \mathbf{B}^T \boldsymbol{\lambda}) = \mathbf{o}. \quad (70)$$

Further substituting (69) into the second equation in (65) we arrive at

$$-\mathbf{B} \mathbf{K}^\dagger \mathbf{B}^T \boldsymbol{\lambda} + \mathbf{B} \mathbf{R} \boldsymbol{\alpha} = -\mathbf{B} \mathbf{K}^\dagger \mathbf{f}. \quad (71)$$

Summarizing (71) and (70) we find that the pair $(\boldsymbol{\lambda}, \boldsymbol{\alpha}) \in \mathbb{R}^{\mathbf{m}} \times \mathbb{R}^l$ satisfies:

$$\begin{pmatrix} \mathbf{F} & \mathbf{N}^T \\ \mathbf{N} & \mathbf{0} \end{pmatrix} \begin{pmatrix} \boldsymbol{\lambda} \\ \boldsymbol{\alpha} \end{pmatrix} = \begin{pmatrix} \mathbf{d} \\ \mathbf{e} \end{pmatrix}, \quad (72)$$

where $\mathbf{F} := \mathbf{B} \mathbf{K}^\dagger \mathbf{B}^T$, $\mathbf{N} := -\mathbf{R}^T \mathbf{B}^T$, $\mathbf{d} := \mathbf{B} \mathbf{K}^\dagger \mathbf{f}$, and $\mathbf{e} := -\mathbf{R}^T \mathbf{f}$

Since \mathbf{N} is of full row-rank as follow from (67), the inverse $(\mathbf{N} \mathbf{N}^T)^{-1}$ exists and $\mathbf{P}_{\mathbf{N}} := \mathbf{I} - \mathbf{N}^T (\mathbf{N} \mathbf{N}^T)^{-1} \mathbf{N}$ is well defined and represents the orthogonal projector onto $\text{Ker} \mathbf{N}$. Applying $\mathbf{P}_{\mathbf{N}}$ on the first equation in (72) and checking that $\mathbf{P}_{\mathbf{N}} \mathbf{N}^T \boldsymbol{\alpha} = \mathbf{o}$ we eliminate $\boldsymbol{\alpha}$ and obtain that $\boldsymbol{\lambda}$ satisfies:

$$\mathbf{P}_{\mathbf{N}} \mathbf{F} \boldsymbol{\lambda} = \mathbf{P}_{\mathbf{N}} \mathbf{d}, \quad \mathbf{N} \boldsymbol{\lambda} = \mathbf{e}. \quad (73)$$

In practical computations, we further decompose $\boldsymbol{\lambda} = \boldsymbol{\lambda}_{\text{Im}} + \boldsymbol{\lambda}_{\text{Ker}}$ into two orthogonal components $\boldsymbol{\lambda}_{\text{Im}} \in \text{Im} \mathbf{N}^T$ and $\boldsymbol{\lambda}_{\text{Ker}} \in \text{Ker} \mathbf{N}$, substitute them in to (73) and get the problem

$$\mathbf{P}_{\mathbf{N}} \mathbf{F} \boldsymbol{\lambda}_{\text{Ker}} = \mathbf{P}_{\mathbf{N}} (\mathbf{d} - \mathbf{F} \boldsymbol{\lambda}_{\text{Im}}) \text{ on } \text{Ker} \mathbf{N}, \quad (74)$$

with $\boldsymbol{\lambda}_{\text{Im}} = \mathbf{N}^T (\mathbf{N} \mathbf{N}^T)^{-1} \mathbf{e}$. Equation (74) is solved efficiently by the projected conjugate gradient method with preconditioning (PCGP) [FMR94] using the lumped preconditioner to \mathbf{F} in the form $\overline{\mathbf{F}}^{-1} = \mathbf{B} \mathbf{K} \mathbf{B}^T$. For more information see [FMR94]. We obtain the following algorithmic scheme for the solution of (62):

Algorithm 3 (Linear solver based on the TFETI method).

- 1: Set $\mathbf{N} := -\mathbf{R}^T \mathbf{B}^T$, $\mathbf{H} := (\mathbf{N} \mathbf{N}^T)^{-1}$, $\mathbf{d} := \mathbf{B} \mathbf{K}^\dagger \mathbf{f}$, and $\mathbf{e} := -\mathbf{R}^T \mathbf{f}$.
- 2: Compute $\boldsymbol{\lambda}_{Im} := \mathbf{N}^T \mathbf{H} \mathbf{e}$.
- 3: Set $\tilde{\mathbf{d}} := \mathbf{d} - \mathbf{F} \boldsymbol{\lambda}_{Im}$.
- 4: Compute $\boldsymbol{\lambda}_{Ker}$ from (74) by PCGP:
- 5: $\mathbf{r}^0 = \tilde{\mathbf{d}}$, $\boldsymbol{\lambda}_{Ker}^0 = \mathbf{o}$.
- 6: **for** $j = 1, 2, \dots$, until convergence **do**
- 7: Project $\mathbf{w}^{j-1} = \mathbf{P}_N \mathbf{r}^{j-1}$.
- 8: Precondition $\mathbf{z}^{j-1} = \overline{\mathbf{F}^{-1}} \mathbf{w}^{j-1}$.
- 9: Re-project $\mathbf{y}^{j-1} = \mathbf{P}_N \mathbf{z}^{j-1}$.
- 10: $\boldsymbol{\beta}^j = (\mathbf{y}^{j-1})^T \mathbf{w}^{j-1} / (\mathbf{y}^{j-2})^T \mathbf{w}^{j-2}$ ($\boldsymbol{\beta}^1 = 0$).
- 11: $\mathbf{p}^j = \mathbf{y}^{j-1} + \boldsymbol{\beta}^j \mathbf{p}^{j-1}$ ($\mathbf{p}^1 = \mathbf{y}^0$).
- 12: $\boldsymbol{\gamma}^j = (\mathbf{y}^{j-1})^T \mathbf{w}^{j-1} / (\mathbf{p}^j)^T \mathbf{F} \mathbf{p}^j$.
- 13: $\boldsymbol{\lambda}_{Ker}^j = \boldsymbol{\lambda}_{Ker}^{j-1} + \boldsymbol{\gamma}^j \mathbf{p}^j$.
- 14: $\mathbf{r}^j = \mathbf{r}^{j-1} - \boldsymbol{\gamma}^j \mathbf{F} \mathbf{p}^j$.
- 15: **if** $\|\mathbf{w}^{j-1}\| \leq \epsilon_{PCGP} \|\mathbf{r}^0\|$ **then stop**.
- 16: **end for**
- 17: $\boldsymbol{\lambda}_{Ker} = \boldsymbol{\lambda}_{Ker}^j$.
- 18: Set $\boldsymbol{\lambda} := \boldsymbol{\lambda}_{Im} + \boldsymbol{\lambda}_{Ker}$.
- 19: Compute $\boldsymbol{\alpha} := \mathbf{H} \mathbf{N} (\mathbf{d} - \mathbf{F} \boldsymbol{\lambda})$.
- 20: Compute $\mathbf{u} := \mathbf{K}^\dagger (\mathbf{f} - \mathbf{B}^T \boldsymbol{\lambda}) + \mathbf{R} \boldsymbol{\alpha}$.

Remark 3. Action of \mathbf{H} on a vector may be efficiently implemented by the sparse Cholesky factorization of $\mathbf{N} \mathbf{N}^T$.

4.3 TFETI based algorithms for solving elastoplastic problem

In this subsection, we summarize the above proposed algorithms for solving elastoplastic problems and modify them with respect to the use of the TFETI domain decomposition method.

Algorithm 4 (Algorithm for solving elastoplastic problem - sequential version).

- 1: $\mathbf{u}_0 = \mathbf{o}$, $\boldsymbol{\sigma}_{0,T} = \mathbf{o}$, $\boldsymbol{\kappa}_{0,T} = \mathbf{o}$, $T \in \mathcal{T}_h$ (initial step)
- 2: **for** $k = 0, 1, 2, \dots, N - 1$ (time steps) **do**
- 3: set $\Delta \mathbf{u}_{k+1,0} = \mathbf{o}$ (zero approximation)
- 4: **for** $i = 1, 2, \dots$ (Newton iterations) **do**
- 5: **for** $p = 1, 2, \dots, s$ (cycle over subdomains) **do**
- 6: restrict $\Delta \mathbf{u}_{k+1,i-1}, \Delta \mathbf{f}_{k+1}$ into subdomain variables $\Delta \mathbf{u}_{k+1,i-1}^p, \Delta \mathbf{f}_{k+1}^p$
- 7: call Algorithm 5 with $(\Delta \mathbf{u}_{k+1,i-1}^p, \Delta \mathbf{f}_{k+1}^p, \boldsymbol{\sigma}_{k,T}, \boldsymbol{\kappa}_{k,T}, T \in \mathcal{T}_h^p)$ to find output variables $\mathbf{K}_{k,i}^p, \mathbf{f}_{k,i}^p, \Delta \boldsymbol{\sigma}_{k+1,T}, \Delta \boldsymbol{\kappa}_{k+1,T}, T \in \mathcal{T}_h^p$.
- 8: collect $\mathbf{K}_{k,i}^p, \mathbf{f}_{k,i}^p$, into global variables $\mathbf{K}_{k,i}, \mathbf{f}_{k,i}$
- 9: **end for** (cycle over subdomains)
- 10: solve by Algorithm 3 the problem: find $\delta \mathbf{u}_i \in \mathbf{V}$ such that

$$\mathbf{J}_{k,i}(\delta \mathbf{u}_i) \leq \mathbf{J}_{k,i}(\mathbf{v}) \quad \forall \mathbf{v} \in \mathbf{V}, \quad \text{with } \mathbf{J}_{k,i}(\mathbf{v}) = \frac{1}{2} \mathbf{v}^T \mathbf{K}_{k,i} \mathbf{v} - \mathbf{f}_{k,i}^T \mathbf{v}$$

- 11: $\Delta \mathbf{u}_{k+1,i} = \Delta \mathbf{u}_{k+1,i-1} + \delta \mathbf{u}_i$ (displacement update)

```

12:   if  $\|\Delta \mathbf{u}_{k+1,i} - \Delta \mathbf{u}_{k+1,i-1}\| / (\|\Delta \mathbf{u}_{k+1,i}\| + \|\Delta \mathbf{u}_{k+1,i-1}\|) \leq \epsilon_{Newton}$  then stop
13: end for(Newton iter.)
14:  $\mathbf{u}_{k+1} = \mathbf{u}_k + \Delta \mathbf{u}_{k+1,i}$ ,
15:  $\boldsymbol{\sigma}_{k+1,T} = \boldsymbol{\sigma}_{k,T} + \Delta \boldsymbol{\sigma}_{k+1,T}$ ,  $\boldsymbol{\kappa}_{k+1,T} = \boldsymbol{\kappa}_{k,T} + \Delta \boldsymbol{\kappa}_{k+1,T}$ ,  $T \in \mathcal{T}_h$ 
16: end for (cycle over time steps)

```

The assembling procedure for subdomain data looks as follows.

Algorithm 5 (Assemble all data corresponding to a subdomain Ω^p).

```

1: Input:  $\Delta \mathbf{u}_{k+1,i-1}^p$ ,  $\Delta \mathbf{f}_{k+1}^p$ ,  $\boldsymbol{\sigma}_{k,T}$ ,  $\boldsymbol{\kappa}_{k,T}$ ,  $T \in \mathcal{T}_h^p$ .
2:  $\mathbf{f}_{k,i}^p = \Delta \mathbf{f}_{k+1}^p$ 
3:  $\mathbf{K}_{k,i}^p = \mathbf{O}$ 
4: for  $T \in \mathcal{T}_h^p$  do
5:   compute  $|T|$  (volume of the element  $T$ )
6:    $\Delta \boldsymbol{\sigma}_{k+1,T} = \mathbf{T}_{k,T} \left( \mathbf{GR}_T^p \Delta \mathbf{u}_{k+1,i-1}^p \right)$ 
7:    $\Delta \boldsymbol{\kappa}_{k+1,T} = \mathbf{T}_{\kappa,k,T} \left( \mathbf{GR}_T^p \Delta \mathbf{u}_{k+1,i-1}^p \right)$ 
8:    $\mathbf{f}_{k,i}^p = \mathbf{f}_{k,i}^p - |T| (\Delta \boldsymbol{\sigma}_{k,T})^T \mathbf{GR}_T^p$ 
9:    $\mathbf{K}_{k,i}^p = \mathbf{K}_{k,i}^p + |T| \left( \mathbf{T}_{k,T}^o \left( \mathbf{GR}_T^p \Delta \mathbf{u}_{k+1,i-1}^p \right) \mathbf{GR}_T^p \right)^T \mathbf{GR}_T^p$ 
10: end for (cycle over elements)
11: Output:  $\mathbf{K}_{k,i}^p$ ,  $\mathbf{f}_{k,i}^p$ ,  $\Delta \boldsymbol{\sigma}_{k+1,T}$ ,  $\Delta \boldsymbol{\kappa}_{k+1,T}$ ,  $T \in \mathcal{T}_h^p$ 

```

Loop over subdomains and all subdomain operations may be implemented in parallel. Parallelization of FETI/TFETI is based on distributing matrix portions among processing units. This allows algorithms to be almost the same in sequential and parallel versions; only data structure implementation differs. Most of computations (subdomain operations) appearing are purely local and therefore parallelizable without any data transfers. Each of cores works with the local part associated with its subdomains. Natural effort using the massively parallel computers is to maximize the number of subdomains so that the sizes of the subdomain stiffness matrices are reduced. This accelerates their factorization and subsequent pseudoinverse application which belongs to the most time consuming action. On the other hand, negative effect of that is an increase of the null space dimension and the number of Lagrange multipliers. This leads to larger coarse problems, i.e., applications of the projector \mathbf{P}_N which are scalable only up to a few thousands of cores and then the coarse problem solution starts to dominate. For the numerical solution of such large problems we recommend to use a hybrid FETI method.

5 Numerical experiments

The performance of the proposed algorithms is demonstrated on an elastoplastic homogeneous thin plate of sizes $20 \times 20 \times 2$ with the circular hole of radius 1 in the center. Its geometry with imposed boundary conditions and indicated symmetry planes is depicted in Figure 3. Thus we consider only eighth of the thin plate in our computations (see Figure 4) and impose symmetry conditions on three symmetry surfaces. A similar benchmark was solved in [St03, GV09, CKM11].

The elastoplastic body Ω is made of homogeneous isotropic material with the parameters

$$E = 206\,900, \nu = 0.29, \sigma_y = 450, \text{ and } H_m = 10\,000,$$

where E and ν are the Young modulus and the Poisson ratio, respectively, which are related with the Lamé coefficients λ and μ by the following formulas:

$$\lambda = \frac{E\nu}{(1+\nu)(1-2\nu)} = 110\,743.8, \quad \mu = \frac{E}{2(1+\nu)} = 801\,938.$$

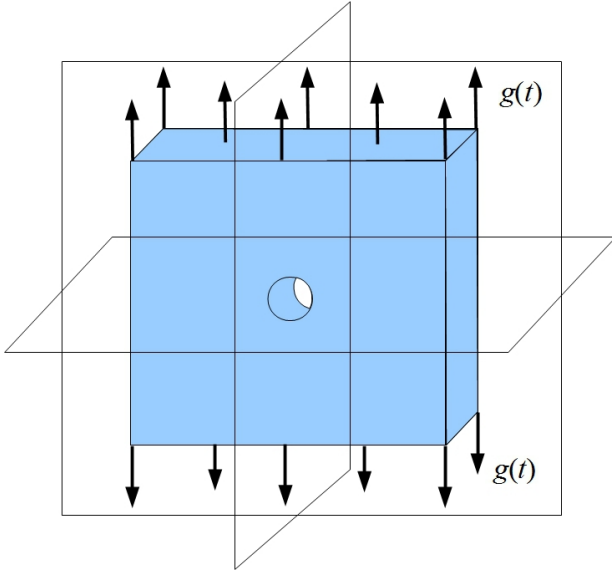


Figure 3: Geometry of the whole body

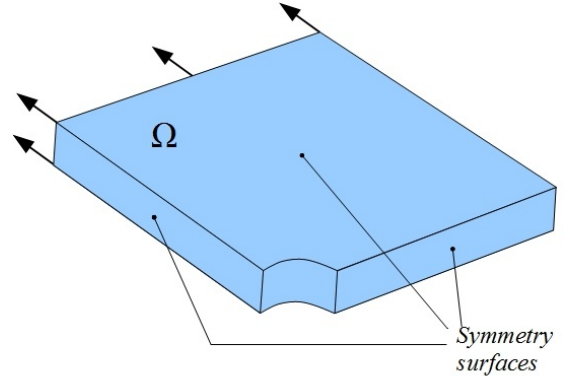


Figure 4: Geometry of eighth of body

The indicated traction forces with the history of loading taking into account are prescribed by the function

$$g(t) = 400 \sin(2\pi t), \quad t \in [t_0, t^*], \quad t_0 = 0, \quad t^* = \frac{1}{4}.$$

Since the elastoplastic model is rate-independent and any local unloading is not expected with respect to the prescribed load history, the results should be independent of the chosen time discretization. Let us consider two variants of the equidistant time discretization characterized by the time step Δt :

- (a) $\Delta t = 1/4, N = 1,$
- (b) $\Delta t = 1/32, N = 8.$

For the spatial discretization of Ω , let us consider five levels of tetrahedral meshes generated by Ansys with

$$520, 1\,623, 9\,947, 166\,374, \text{ and } 309\,546$$

nodes decomposed into subdomains using Metis. An example of such decomposition is depicted in Figure 5 and a zoom near the hole in Figure 6.

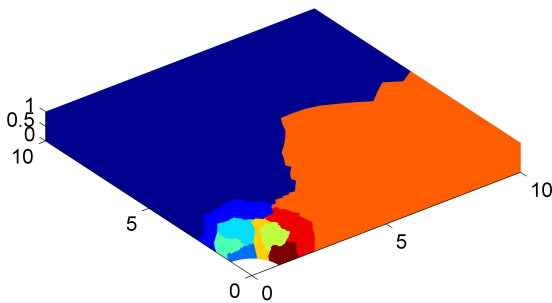


Figure 5: Domain decomposition into 10 subdomains

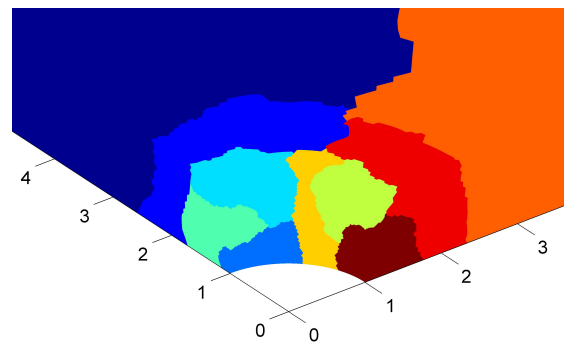


Figure 6: Zoom of Figure 5 near the hole

The proposed algorithms were implemented in `MatSol` library [KMBKVD09] developed in Matlab and parallelized using Matlab Distributed Computing Server and Matlab Parallel Toolbox. For all computations

we use maximum 28 cores with 2GB memory per core of the HP Blade system, model BLc7000. The stopping tolerances of the Newton and the PCGP algorithms are

$$\epsilon_{Newton} = 10^{-4} \text{ and } \epsilon_{PCGP} = 10^{-7}, \quad (75)$$

respectively.

In Table 1, we report the numerical results for the time discretization (a) and different mesh levels. The numbers of subdomains are chosen to keep the number of nodes per subdomain approximately constant except the coarsest mesh level. We see that the number of the Newton iterations remains almost constant for all meshes. Similar behavior was observed in the numerical results by [GV09]. Note that even the number of the PCGP iterations increases only moderately for larger meshes. In Table 2, the number of the PCGP iterations, the number of plastic elements, and the relative convergence criterion are reported for each Newton's iteration of Algorithm 4, the time discretization (a), and the finest mesh level. In this case, we set the stopping tolerances $\epsilon_{Newton} = 10^{-9}$ and $\epsilon_{PCGP} = 10^{-14}$ so accurate to observe quadratic convergence of the Newton method after identification of the plastic zone. Such behavior agrees with the theoretical results in [B199].

The computational history of Algorithm 4 for the time discretization (b), the finest mesh level, and the stopping tolerances (75) is documented in Table 3. The corresponding development of the plastic zone is depicted for the times $t_2, t_4, t_6,$ and t_8 in Figures 7 - 10, respectively. The growing zone of plastic elements results from the monotonically increased loading. Distributions of the von Mises stress $\|\text{dev}(\sigma)\|_F$ and the total displacement $\|u\|$ at the final time t^* are depicted in Figures 11 and 12, respectively.

Mesh level	1	2	3	4	5
Number of mesh nodes	520	1 623	9 947	166 374	309 546
Number of mesh elements	1 441	6 279	48 287	931 709	1 758 907
Number of subdomains	1	1	8	135	270
Number of CPU cores	2	2	9	28	28
Number of primal variables	1 560	4 869	33 414	623 904	1 183 101
Number of dual variables	284	618	5 448	136 904	272 053
Number of plastic elements	252	2 152	20 790	420 760	796 520
Number of Newton iterations.	5	6	6	6	6
Total number of PCGP iterations	237	391	573	718	724
Total time in seconds	8	60	77	928	1796

Table 1: Numerical results of Algorithm 4 for different mesh levels and the time discretization (a).

Newton iter.	Number of PCGP iters.	Number of plastic elem.	Stopping criterion
1	224	0	1
2	312	808 116	1.4016e-1
3	310	797 081	4.6051e-2
4	319	788 802	6.3207e-3
5	318	795 245	4.5604e-4
6	319	796 519	1.0735e-5
7	321	796 596	1.1790e-8
8	314	796 596	9.0488e-14

Table 2: Computational history of Algorithm 4 for the time discretization (a) and the finest mesh level

Remark 4. The numbers of the PCGP iterations may be decreased by reducing the required accuracy or by assuming the inexact Newton method [B199].

Comparing time discretizations (a) and (b) we see that the resulting number of plastic elements differs at the final time t^* . The difference is less than 0.5% and is caused by the roundoff errors, the use of iterative solvers, and the numerical evaluation of the yield function which decides whether an element plasticizes or not.

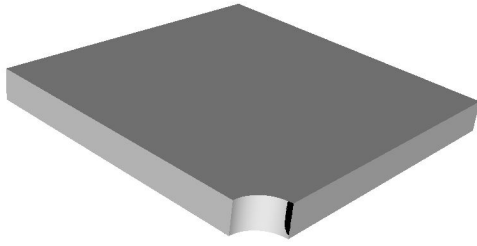


Figure 7: Elastic (gray color) and plastic (black color) elements at time t_2

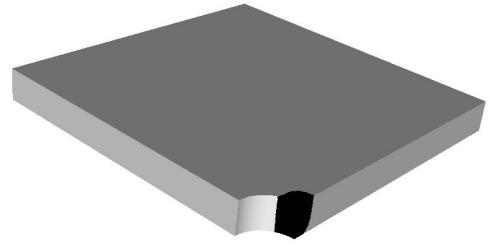


Figure 8: Elastic (gray color) and plastic (black color) elements at time t_4

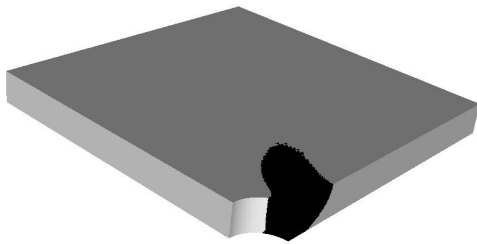


Figure 9: Elastic (gray color) and plastic (black color) elements at time t_6

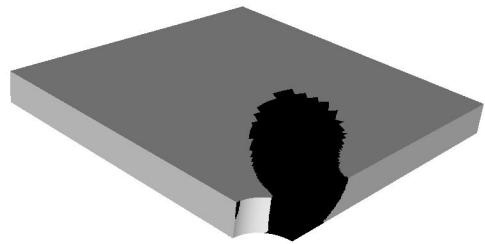


Figure 10: Elastic (gray color) and plastic (black color) elements at time t_8

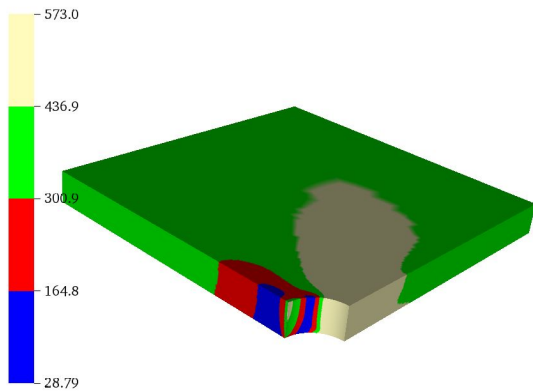


Figure 11: Distribution of von Mises stress $\|\text{dev}(\sigma)\|_F$ at t_8

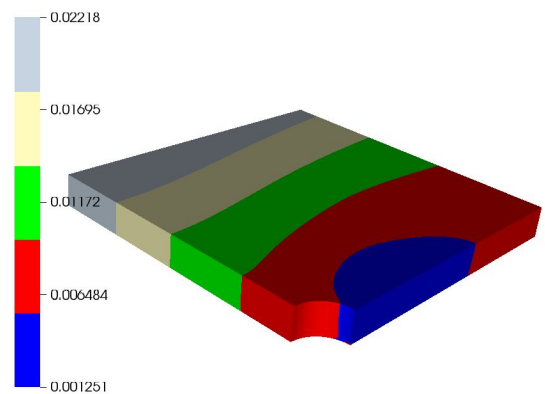


Figure 12: Total displacement $\|u\|$ at t_8

Time step	Number of Newton iters.	Total number of PCGP iterations	Number of plastic elems.	Solution time
1	2	226	0	536
2	2	228	8 700	534
3	4	487	181 557	1 152
4	4	522	316 718	1 237
5	4	553	502 605	1 270
6	5	863	671 067	1 678
7	5	899	762 501	1 638
8	4	662	799 989	1 445

Table 3: Computational history of Algorithm 4 for the time discretization (b) and the finest mesh level

6 Conclusion

We have proposed the algorithm for the efficient parallel implementation of elastoplastic problems with the von Mises plastic criterion and the linear isotropic hardening law which is based on the TFETI domain decomposition method. For the time discretization we used implicit Euler method and for the space discretization of the respective one time step elastoplastic problem the finite element method. The latter results in a system of nonlinear equations with a strongly semismooth and strongly monotone operator. Thus the semismooth Newton method was applied and respective linearized problems were solved in parallel using TFETI.

The performance of our algorithm was demonstrated on the 3D elastoplastic thin plate with the hole in the center and prescribed loading history. Numerical results for different time discretizations and mesh levels were presented and discussed. Local quadratic convergence of the semismooth Newton method was observed after identification of the plastic zone which is in accordance with the theoretical results. Our future plan is to apply the proposed TFETI based algorithm on elastoplastic multi-body contact problems of mechanics. This has already been done successfully for the pure elastic case [DKVBM10, DKMBVH12].

Acknowledgements

This work was supported by the European Regional Development Fund in the IT4Innovations Centre of Excellence project (CZ.1.05/1.1.00/02.0070) and by the project SPOMECH - Creating a multidisciplinary R&D team for reliable solution of mechanical problems, reg. no. CZ.1.07/2.3.00/20.0070 within Operational Programme 'Education for competitiveness' funded by Structural Funds of the European Union and state budget of the Czech Republic. Authors would particularly like to thank to T. Brzobohaty and A. Markopoulos from CE IT4Innovations, VSB-TU Ostrava for generating different finite element meshes and advices concerning Matsol implementation.

References

- [ACFK02] Albery, J., Carstensen, C., Funken, S.A., Klose, R., *Matlab implementation of the finite element method in elasticity* Computing (Vienna/New York) 69 (3) , 239–263, 2002.
- [ACZ99] Albery J., Carstensen C., Zarrabi D., *Adaptive numerical analysis in primal elastoplasticity with hardening*, Comput. Methods Appl. Mech. Engrg. 171, 175-204, 1999.
- [BG94] Badea, L., Gilormini, P., *Application of a domain decomposition method to elastoplastic problems*, International Journal of Solids and Structures 31 (5), Pages 643656, 1994.
- [BGL05] Benzi, M., Golub, G. H., Liesen, J., *Numerical solution of saddle point problems*, Acta Numerica, 1–137, Cambridge University Press, 2005.
- [Bl99] Blaheta, R., *Numerical methods in elasto-plasticity*, Documenta Geonica 1998, PERES Publishers, Prague, 1999.

- [BS96] Brokate, M., Sprekels J., *Hysteresis and Phase Transitions*, Springer-Verlag New York, 1996.
- [BDKKM10] Brzobohatý, T., Dostál, Z., Kovář, P., Kozubek, T., Markopoulos, A. *Cholesky decomposition with fixing nodes to stable evaluation of a generalized inverse of the stiffness matrix of a floating structure*, International Journal for Numerical Methods in Engineering 88 (5), 493–509, 2011.
- [C93] Carstensen C., *Nonlinear Interface Problems in Solid Mechanics: Finite Element and Boundary Element Couplings*, habilitation thesis, University Hannover, 1993.
- [CK02] Carstensen, C., Klose, R., *Elastoviscoplastic finite element analysis in 100 lines of Matlab* Journal of Numerical Mathematics 10 (3) , 157–192, 2002.
- [CKM11] Čermák, M., Kozubek, T., Markopoulos, A., *An efficient FETI based solver for elasto-plastic problems of mechanics*, Computational Plasticity XI - Fundamentals and Applications, COMPLAS XI, 1330–1341, 2011.
- [D09] Dostál, Z., *Optimal Quadratic Programming Algorithms, with Applications to Variational Inequalities*, SOIA 23, Springer US, New York, 2009.
- [DHK06] Dostál, Z., Horák, D., Kučera, R., *Total FETI - an easier implementable variant of the FETI method for numerical solution of elliptic PDE*, Communications in Numerical Methods in Engineering 22 (12), 1155–1162, 2006.
- [DKMBVH12] Dostál, Z., Kozubek, T., Markopoulos, A., Brzobohatý, T., Vondrák, V., Horyl, P., *Theoretically supported scalable TFETI algorithm for the solution of multibody 3D contact problems with friction*, Comput Method Appl M 205–208, 110–120, 2012.
- [DKVBM10] Dostál, Z., Kozubek, T., Vondrák, V., Brzobohatý, T., Markopoulos, A., *Scalable TFETI algorithm for the solution of multibody contact problems of elasticity*, Int J Numer Meth Eng 82, 1384–1405, 2010.
- [FMR94] Farhat, C., Mandel, J., Roux, F-X., *Optimal convergence properties of the FETI domain decomposition method*, Computer Methods in Applied Mechanics and Engineering 115, 365–385, 1994.
- [FR92] Farhat, C., Roux, F-X., *An unconventional domain decomposition method for an efficient parallel solution of large-scale finite element systems*, SIAM J. Sci. Stat. Comput. 13, 379–396, 1992.
- [FK80] Fučík, S., Kufner, A., *Nonlinear Differential Equation*, Elsevier, Amsterdam, 1980.
- [GKLSV11] Gruber P., Kienesberger J., Langer U., Schoeberl J., Valdman J., *Fast solvers and a posteriori error estimates in elastoplasticity*, U. Langer and P. Paule (editors), Numerical and Symbolic Scientific Computation: Progress and Prospects, Texts and Monographs in Symbolic Computation, Wien: Springer, 45–63, 2011.
- [GV09] Gruber, P., Valdman, J., *Solution of One-Time Step Problems in Elastoplasticity by a Slant Newton Method*, SIAM J. Sci. Comp. 31, 1558–1580, 2009.
- [HR99] Han, W., Reddy B. D., *Plasticity: mathematical theory and numerical analysis*, Springer, 1999.
- [Jo76] Johnson C., *Existence theorems for plasticity problems*, J. Math. pures et appl. 55, 431-444, 1976.
- [Jo78] Johnson C., *On plasticity with hardening*, J. Math. Anal. Appl. 62, 325-336, 1978.
- [KLV04] Kienesberger J., Langer U., Valdman J., *On a robust multigrid-preconditioned solver for incremental plasticity problems*, Proceedings of IMET 2004 - Iterative Methods, Preconditioning & Numerical PDEs, Prague.
- [KL84] Korneev V.G., Langer U., *Approximate solution of plastic flow theory problems*, Teubner-Verlag, Leipzig, volume 69, 1984.

- [KMBKVD09] Kozubek, T., Markopoulos, A., Brzobohatý, T., Kučera, R., Vondrák, V., Dostál, Z. *MatSol - MATLAB efficient solvers for problems in engineering*, <http://matsol.vsb.cz/>.
- [KVMHDKC12] Kozubek, T., Vondrák, V., Menšík M., Horák D., Dostál, Z., Hapla V., Kabelíková P., Čermák M., *Total FETI domain decomposition method and its massively parallel implementation*, Computers and Structures, 2012, submitted.
- [Kr96] Krejčí P., *Hysteresis, Convexity and Dissipation in Hyperbolic Equations*, GAKUTO International Series, Mathematical Sciences and Applications (1996).
- [Ma79] Matthies, H., *Existence theorems in thermoplasticity*, J. Mecanique 18 (1979), No. 4, 695-712.
- [Ma79b] Matthies, H., *Finite element approximations in thermo-plasticity*, Numer. Funct. Anal. Optim. 1 (1979), No. 2, 145-160.
- [Mi77] Mifflin, R., *Semismoothness and semiconvex function in constraint optimization*, SIAM Journal on Control and Optimization 15, 957-972, 1977.
- [NH81] Nečas, J., Hlaváček, I., *Mathematical Theory of Elastic and Elasto-Plastic Bodies. An Introduction*, Elsevier, Amsterdam, 1981.
- [QS93] Qi, L., Sun, J., *A nonsmooth version of Newtons method*, Mathematical Programming, 58, 353-367, 1993.
- [Ro92] Roux, F-X., *Spectral analysis of interface operator*, Proceedings of the 5th Int. Symp. on Domain Decomposition Methods for Partial Differential Equations, ed. D. E. Keyes et al., SIAM, 73-90, Philadelphia 1992.
- [RF98] Roux, F-X., Farhat, C., *Parallel implementation of direct solution strategies for the coarse grid solvers in 2-level FETI method*, Contemporary Math. 218, 158-173, 1998.
- [SW11] Sauter M., Wieners C., *On the superlinear convergence in computational elasto-plasticity*, Comp. Meth. Eng. Mech. 200, 3646-3658, (2011)
- [SH98] Simo, J. C., Hughes, T. J. R., *Computational Inelasticity*, Interdiscip. Appl. Math. 7, Springer-Verlag, New York, 1998.
- [NPO08] de Souza Neto, E. A., Perić, D., Owen, D. R. J., *Computational methods for plasticity: theory and application*. Wiley, 2008.
- [St03] Stein, E. et al., *Error-Controlled Adaptive Finite Elements in Solid Mechanics*, Wiley, Chichester, UK, 2003.
- [Sy09] Sysala, S., *Application of a modified semismooth Newton method to some elasto-plastic problems*. Submitted to Math. Comp. Sim. in 2009.
- [Sy12] Sysala, S., *Properties and simplifications of constitutive time-discretized elastoplastic operators*. Submitted to ZAMM journal in 2012.
- [Wi00] Wieners, C., *Multigrid methods for finite elements and the application to solid mechanics. Theorie und Numerik der Prandtl-Reuß Plastizität*, habilitation thesis, University Heidelberg, 2000.
- [Wi10] Wieners, C., *A geometric data structure for parallel finite elements and the application to multigrid methods with block smoothing*, Computing and Visualization in Science 13 (4), 161-175, 2010.